

# An efficient Equilibrium Optimizer for parameters identification of photovoltaic modules

Essam H. Houssein<sup>1</sup>, Gamela Nageh<sup>1</sup>, Mohamed Abd Elaziz<sup>2</sup> and Eman Younis<sup>1</sup>

<sup>1</sup> Faculty of Computers and Information, Minia University, Minia, Egypt

<sup>2</sup> Department of Mathematics, Faculty of Science, Zagazig University, Zagazig, Egypt

## ABSTRACT

The use of solar photovoltaic systems (PVs) is increasing as a clean and affordable source of electric energy. The PV cell is the main component of the PV system. To improve the performance, control, and evaluation of the PV system, it is necessary to provide accurate design and to define the intrinsic parameters of the solar cells. There are many methods for optimizing the parameters of the solar cells. The first class of methods is called the analytical methods that provide the model parameters using datasheet information or I-V curve data. The second class of methods is the optimization-based methods that define the problem as an optimization problem. The optimization problem objective is to minimize the error metrics and it is solved using metaheuristic optimization algorithms. The third class of methods is composed of a hybrid of both the analytical and the metaheuristic approaches, some parameters are computed by the analytical approach and the rest are found using metaheuristic optimization algorithms. Research in this area faces two challenges; (1) finding an optimal model for the parameters of the solar cells and (2) the lack of data about the photovoltaic cells. This paper proposes an optimization-based algorithm for accurately estimating the parameters of solar cells. It is using the Improved Equilibrium Optimizer algorithm (IEO). This algorithm is improved using the Opposition Based Learning (OBL) at the initialization phase of EO to improve its population diversity in the search space. Opposition-based Learning (OBL) is a new concept in machine learning inspired by the opposite relationship among entities. There are two common models for solar cells; the single diode model (SDM) and double diode model (DDM) have been used to demonstrate the capabilities of IEO in estimating the parameters of solar cells. The proposed methodology can find accurate solutions while reducing the computational cost. Compared to other existing techniques, the proposed algorithm yields less mean absolute error. The results were compared with seven optimization algorithms using data of different solar cells and PV panels. The experimental results revealed that IEO is superior to the most competitive algorithms in terms of the accuracy of the final solutions.

Submitted 11 December 2020  
Accepted 17 August 2021  
Published 9 September 2021

Corresponding author  
Gamela Nageh,  
gamela.nageh@mu.edu.eg

Academic editor  
Chan Hwang See

Additional Information and  
Declarations can be found on  
page 26

DOI [10.7717/peerj.cs.708](https://doi.org/10.7717/peerj.cs.708)

© Copyright  
2021 Houssein et al.

Distributed under  
Creative Commons CC-BY 4.0

## OPEN ACCESS

**Subjects** Algorithms and Analysis of Algorithms, Artificial Intelligence, Optimization Theory and Computation

**Keywords** Improve equilibrium optimizer algorithm (IEO), PV parameter estimation, Opposition based learning (OBL), Single diode model (SDM), Double diode model (DDM), Solar energy

## INTRODUCTION

A major drawback of the use of fossil fuel is its negative environmental effects; therefore, alternative renewable energy sources (RESs) are used as an alternative clean and affordable energy source. There are seven types of RESs namely, biomass ([López et al., 2008](#)), geothermal ([Houssein, 2019](#)), wind ([Osama et al., 2017](#)), solar ([Hocaoglu, 2011; Munshi & Yasser, 2017](#)), hydroelectric ([Bagher et al., 2015](#)), hydrogen ([Dunn, 2002](#)), and tide ([Egbert & Ray, 2000](#)). Solar energy is considered one of the most important sources of renewable energy, as the sun plays a significant role in its generation. A PV system uses solar cells (SCs) to convert the sunlight into electricity ([AbdElminaam, Said & Houssein, 2021](#)).

PV SCs are a type of RES that is clean (*i.e.*, generates no pollution), has a long life, has a simple design and easy to install. However, solar energy has several drawbacks compared with other RES. The main disadvantages of PV solar energy systems are the high initial exploitation and low capacity of SCs ([Navabi et al., 2015](#)). An open research topic is optimizing the efficiency of SCs. Because PV modules are installed outdoors, the weather conditions affect the generated energy, which results in a high maintenance cost and difficulty in control.

PV modules contain SCs, which consist of a semiconductor of monocrystalline material (KC200GT) ([Park et al., 2014](#)), monocrystalline (SM55) ([Salam, Ishaque & Taheri, 2010](#)), and thin film (ST40) ([Alam, Yousri & Eteiba, 2015](#)). The global settings of a SC depend on a circuit to examine the performance of the cell under various conditions, such as temperature and solar irradiance. A SC can be described by the following two popular models: the single-diode model (SDM) and the double-diode model (DDM) ([Lim et al., 2015; Humada et al., 2016; Ismaeel et al., 2021](#)). The SDM is similar to the DDM, and the variation in cellular performance is imperceptible. The SDM is more common than the DDM. The SDM model includes five unknown parameters, while the DDM has seven unknown parameters. Accurate determination of the unknown variables plays an important role in optimizing the SC and its internal parameters.

The PV module manufacturer's data sheet contains the parameters of the open circuit voltage ( $V_{oc}$ ), voltage and current at the point of maximum power ( $V_{mppt}$  and  $I_{mppt}$ ), short-circuit current ( $I_{sc}$ ), maximum power ( $P_{mppt}$ ), voltage temperature and current temperature coefficients ( $K_v$  and  $K_i$ ). These parameters can also be obtained experimentally. The SDM, however, requires other parameters, such as the reverse saturation current ( $I_0$ ), photogenerated current ( $I_{pv}$ ), nonphysical ideality factor of the diode ( $a$ ), shunt resistance ( $R_p$ ), and series resistance ( $R_s$ ). However, these parameters are not provided in the data sheet. Therefore, determining these parameters is a major research challenge.

There are three types of approaches for solving the parameter estimation problem: traditional methods (analytical methods) ([Easwarakhanthan et al., 1986](#)), metaheuristic methods ([AlRashidi et al., 2011](#)) and hybrid methods. Traditional methods use a modified nonlinear least squares estimation approach based on Newton's method. Traditional approaches depend on the starting point of the iterative method, which is a key problem.

As a result, these methods tend to be trapped in local solutions. An example of this type of techniques is presented in [Chan, Phillips & Phang \(1986\)](#). Several features, such as convexity, continuity, and differentiability, are required for usability. The drawbacks of these methods include high demand of computational resources, sensitivity to initial conditions, and the tendency to provide sub-optimal solutions.

Unlike conventional methods, metaheuristic approaches have been proposed to increase the probability of obtaining the global solution in a reasonable time. In the literature, the problem of determining the parameters of the SC has been solved using genetic algorithms (GA) ([Ismail, Moghavvemi & Mahlia, 2013](#)), particle swarm optimization (PSO) ([Wei et al., 2011](#)), and simulated annealing (SA) ([El-Naggar et al., 2012](#)). Although these metaheuristic algorithms produce better solutions than conventional algorithms, they have some limitations ([Dai, Chen & Zhu, 2009](#)). The third approach for solving this problem is using hybrid methods which use a combination of the analytical and the metaheuristic approaches. A review of the methods of the parameter estimation of the SCs is presented in [Oliva et al. \(2019\)](#).

Recently, researchers have used metaheuristic algorithms to extract the optimal parameters of PV systems ([Oliva et al., 2019](#)). These algorithms include the bird-mating optimizer ([Askarzadeh & Rezazadeh, 2013b](#)), artificial immune system ([Jacob et al., 2015](#)), repaired adaptive differential evolution ([Gong & Cai, 2013](#)), pattern search ([AlHajri et al., 2012](#)), harmony search-based algorithms ([Askarzadeh & Rezazadeh, 2012](#)), SA ([El-Naggar et al., 2012](#)), chaos particle swarm algorithm ([Wei et al., 2011](#)), artificial bee colony ([Askarzadeh & Rezazadeh, 2013a](#)) the mutative-scale parallel chaos optimization algorithm ([Yuan, Xiang & He, 2014](#)), adaptive differential evolution ([Chellaswamy & Ramesh, 2016](#)), gray wolf optimizer (GWO) ([Rodrguez & Murillo, 2017](#)), mine blast algorithm ([El-Fergany, 2015](#)), improved shuffled complex evolution algorithm ([Gao et al., 2018](#)), direct search optimization algorithm ([Osheba, Azazi & Shokralla, 2017](#)), evaporation-rate-based water cycle algorithm ([Gotmare et al., 2017](#)), Tabu search ([Siddiqui & Abido, 2013](#)), and chaos PSO ([Wei et al., 2011](#)).

An interesting approach to solve the problem of solar PV parameter estimation is based on the flower pollination algorithm (FPA) ([Alam, Yousri & Eteiba, 2015](#)). The FPA mimics flower pollination behavior. However, its results are inaccurate. The multi-verse optimizer has also been used to extract the parameters of the PV system. But, this algorithm also generates results far from the optimal solution ([Ali et al., 2016](#)). An optimization algorithm for artificial swarms of bees identifies parameters of the SC models and is inspired by the intelligent behaviors of the bees, such as collecting and processing nectar ([Askarzadeh & Rezazadeh, 2013a](#)). The simplified swarm optimization algorithm (MSSO) has been applied to both the SDM and DDM to minimize the square error between the experimental and calculated data. However, this minimization was not efficient  $9.8607E^{-04}$  ([Lin et al., 2017a](#)). The improved chaotic whale optimization algorithm has also been used to estimate the parameters of the PV. However, it is complex and difficult to apply ([Oliva, El Aziz & Hassanien, 2017](#)). The most recent typologies in the literature are listed in [Table 1](#).

**Table 1** Summary of the previous related research.

Year	Method	RMSE
2017	MSSO ( <a href="#">Lin et al., 2017b</a> )	SDM: $9.8607E^{-04}$ DDM: $9.8281E^{-04}$ %
2017	ABC with chaotic maps ( <a href="#">Oliva et al., 2017</a> )	SDM: $9.8602 \times 10^{-04}$ DDM: $9.8262 \times 10^{-04}$
2017	WDO ( <a href="#">Derick et al., 2017</a> )	SDM: 0.00084 DDM: 0.00106
2017	WOA with chaotic maps ( <a href="#">Oliva, El Aziz &amp; Hassani, 2017</a> )	SDM: $9.8602 \times 10^{-04}$ DDM: $9.8272 \times 10^{-04}$
2018	SCE with a complex evolution strategy ( <a href="#">Gao et al., 2018</a> )	SDM: $9.8602 \times 10^{-04}$ DDM: $9.8248 \times 10^{-04}$
2018	WDO ( <a href="#">Mathew et al., 2017</a> )	DDM: 0.127
2018	ImCSA ( <a href="#">Kang et al., 2018</a> )	SDM: $9.8602E^{-04}$ DDM: $9.8249E^{-04}$
2019	TLO ( <a href="#">Li et al., 2019</a> )	SDM: $9.8609E^{-04}$ DDM: $9.8612E^{-04}$
2019	ISCA ( <a href="#">Chen et al., 2019</a> )	SDM: $9.8602E^{-04}$ DDM: $9.8237E^{-04}$
2020	SMA ( <a href="#">Kumar et al., 2020</a> )	SDM: $9.8582E^{-04}$ DDM: $9.8148E^{-04}$
2020	COA ( <a href="#">Diab et al., 2020</a> )	SDM: $7.7547E^{-04}$ DDM: $7.6480E^{-04}$

The above methods use metaheuristic algorithms that require large computational time and lead to high error rate between the experimental and the calculated data. Therefore, this work proposes an efficient algorithm called the improved equilibrium optimizer (IEO) algorithm to estimate the optimal parameters of the PV system. IEO was validated by comparing its results with those of a mathematical method and other approaches. Using the IEO, the minimum error between the estimated and the experimental data and the minimum convergence time for the optimal parameters and the best curve fit (I-V) was obtained. An accurate PV model based on IEO algorithm can play an important role in increasing the overall efficiency of a PV system. It guarantees the optimal use of the available solar energy, which results in reducing the costs of the PV system. To the best of our knowledge, the IEO is a new optimization algorithm whose potential has not yet been extensively applied in real problems. The motivation of this paper is to propose a parameter estimation technique for efficiently and accurately extracting the parameters of the SCs and PV modules. The major contributions of this work are as follows:

1. Proposing the Improved Equilibrium Optimizer (IEO) algorithm, which is inspired by the control, volume, mass, and balance models for estimating the photovoltaic (PV) parameters.

2. IEO algorithm proved that it can obtain the optimal value of the PV variables of single and double diode models.
3. Comparing the IEO with other metaheuristic algorithms the results show that IEO provided smaller errors between the calculated values and the actual values.

The remainder of this paper is organized as follows: ‘Mathematical Model of Photovoltaic Cell/Module’ offers a depiction of the mathematical model of the PV cell/module. Equilibrium optimizer (EO) and Improved Equilibrium Optimizer (IEO) are presented in ‘Equilibrium Optimizer (EO) Algorithm’ and ‘Improved Equilibrium Optimizer (IEO) Algorithm’, respectively. The modified objective function is introduced in ‘Objective Function’. In ‘Simulation Results and Analysis’ and ‘Results of Comparing the Efficiency of the Ieo with other Metaheuristic Algorithms’ analysis and Comparative study of the proposed algorithm with other meta-heuristics algorithms are provided. Finally, the conclusions and future work are presented in ‘Conclusions and Future Work’.

## MATHEMATICAL MODEL OF PHOTOVOLTAIC CELL/MODULE

This section presents the mathematical model of the PV unit (*Biswas et al., 2019*) that can be obtained by the SDM (*El-Arini, Othman & Fathy, 2013*) and DDM (*Chin et al., 2011*). **Figure 1** displays the equipollent circuit diagram of a typical PV cell. The current ( $I$ ) of this cell is as follows:

$$I = I_{PV,Cell} - I_D \quad (1)$$

where,  $I_{PV,Cell}$  is the PV current and  $I_D$  is the diode current.

$$I_D = I_{O,Cell} \left[ \exp\left(\frac{qV}{aKT}\right) - 1 \right] \quad (2)$$

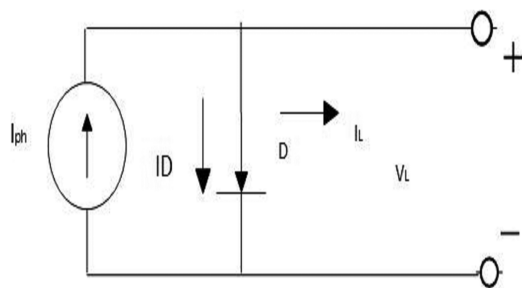
where,  $I_{O,Cell}$  is the reverse saturation current of the diode,  $q$  ( $1.60217646 \times 10^{-19}$  (C)) is the charge of an electron,  $k$  ( $1.38064852 \times 10^{-23}$  J/K) is the Boltzmann constant,  $T$  is the temperature (in Kelvin) of the diode junction, and  $a$  is the ideal factor of the diode. Therefore, **Eq. (1)** can be rewritten to obtain the I-V characteristic of a typical cell as follows:

$$I = I_{PV,Cell} - I_{O,Cell} \left[ \exp\left(\frac{qV}{aKT}\right) - 1 \right] \quad (3)$$

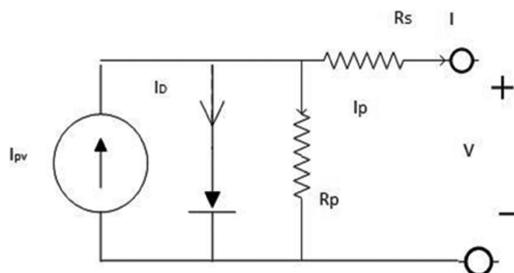
PV cells can be linked either in parallel or in series to form a PV system. Here,  $N_c$  represents the number of cells that are linked in series.

### Single diode model

In the SDM, five unknown parameters must be obtained. These parameters are the photon current ( $I_{pv}$ ), reverse saturation current of the diode ( $I_o$ ), the ideality factor ( $a$ ), and the series and parallel resistances ( $R_s$  and  $R_p$ ). **Figure 2** presents the SDM of a PV cell with  $N_c$  series-connected cells.

**Figure 1** Equivalent circuit of an ideal photovoltaic (PV) cell.

Full-size DOI: 10.7717/peerj-cs.708/fig-1

**Figure 2** Single-diode model of photovoltaic (PV) cell. Full-size DOI: 10.7717/peerj-cs.708/fig-2

Therefore, the  $I$ - $V$  characteristics of the SDM of the PV are represented as:

$$I = I_{PV} - I_O \left[ \exp \left( \frac{q(V + R_S I)}{a K N_C T} \right) - 1 \right] - \frac{V + R_S I}{R_S} \quad (4)$$

At the point of the open circuit, we find that ( $V = V_{OC}$ ) and ( $I = 0$ ) (opinion); thereafter, from Eq. (4), we obtain;

$$0 = I_{PV} - I_O \left[ \exp \left( \frac{q V_{OC}}{a K N_C T} \right) - 1 \right] - \frac{V_{OC}}{R_P} \quad (5)$$

$$\text{Thus, } I_{PV} = I_O \left[ \exp \left( \frac{q V_{OC}}{a K N_C T} \right) - 1 \right] - \frac{V_{OC}}{R_P} \quad (6)$$

At the point of the short circuit ( $I = I_{SC}$ ) and ( $V = 0$ ) (opinion); thereafter, from Eq. (4) we obtain;

$$I_{SC} = I_{PV} - I_O \left[ \exp \left( \frac{q R_S I_{SC}}{a K N_C T} \right) - 1 \right] - \frac{R_S I_{SC}}{R_P} \quad (7)$$

$$\text{Therefore, } I_{PV} = I_{SC} + I_O \left[ \exp \left( \frac{q R_S I_{SC}}{a K N_C T} \right) - 1 \right] - \frac{R_S I_{SC}}{R_P} \quad (8)$$

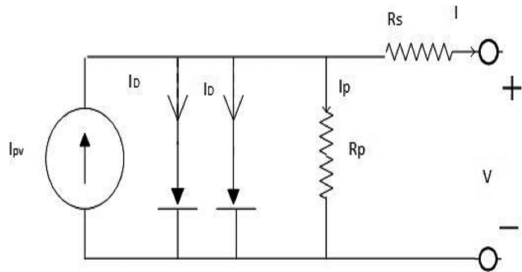


Figure 3 Double diode model of the PVcell.

Full-size DOI: 10.7717/peerj-cs.708/fig-3

From Eqs. (6) and (8) we have;

$$I_O = \frac{I_{SC} + \frac{R_S I_{SC}}{R_P} - \frac{V_{OC}}{R_P}}{\exp\left(\frac{qV_{OC}}{aK_N C T}\right) - \exp\left(\frac{qR_S I_{SC}}{aK_N C T}\right)} \quad (9)$$

Substituting Eq. (9) into Eq. (6) yields;

$$I_{PV} = \frac{\left(I_{SC} + \frac{R_S I_{SC}}{R_P} - \frac{V_{OC}}{R_P}\right) \left[\exp\left(\frac{qV_{OC}}{aK_N C T}\right) - 1\right]}{\exp\left(\frac{qV_{OC}}{aK_N C T}\right) - \exp\left(\frac{qR_S I_{SC}}{aK_N C T}\right)} \quad (10)$$

At the maximum power point ( $V = V_{MPP}$ ) and ( $I = I_{MPP}$ ) (say), from Eq. (4) we have;

$$I_{MPP} = I_{PV} - I_O \left[ \exp \frac{q(V_{MPP} + R_S I_{MPP})}{aK_N C T} - 1 \right] - \frac{V_{MPP} + R_S I_{MPP}}{R_P} \quad (11)$$

### Double-diode model

In the DDM in Fig. 3, seven unknown parameters must be obtained. These parameters are the photon current ( $I_{pv}$ ), reverse saturation current of the first diode ( $I_{O1}$ ), reverse saturation current of second diode ( $I_{O2}$ ), ideality factors of the first and second diodes ( $a_1$ ) and  $a_2$ , and the PV cell series and parallel resistances ( $R_s$  and  $R_p$ ). Therefore, the I-V characteristics of the DDM are as follows:

$$I = I_{PV} - I_{D1} - I_{D2} - \frac{V + R_s I}{R_p} \quad (12)$$

$$\text{i.e., } I = I_{PV} - I_{O1} \left[ \exp \frac{q(V + R_s I)}{a_1 K_N C T} - 1 \right] - I_{O2} \left[ \exp \frac{q(V + R_s I)}{a_2 K_N C T} - 1 \right] - \frac{V + R_s I}{R_p} \quad (13)$$

At the point of the open circuit,  $I = 0$  and  $V = V_{OC}$ ; thus, from Eq. (13) we obtain;

$$0 = I_{PV} - I_{O1} \left[ \exp \frac{q(V + R_s I)}{a_1 K_N C T} - 1 \right] - I_{O2} \left[ \exp \frac{q(V + R_s I)}{a_2 K_N C T} - 1 \right] - \frac{V_{OC}}{R_s} \quad (14)$$

$$\text{Therefore, } I_{PV} = O1 \left[ \exp \frac{q(V + R_S I)}{a_1 k N_C T} - 1 \right] - I_{O2} \left[ \exp \frac{q(V + R_S I)}{a_2 k N_C T} - 1 \right] - \frac{V_{OC}}{R_S} \quad (15)$$

At the point of the short circuit,  $V = 0$  and  $I = I_{SC}$ ; thus, from Eq. (13) we obtain;

$$I_{SC} = I_{PV} - I_{O1} \left[ \exp \left( \frac{q R_S I_{SC}}{a_1 k N_C T} \right) - 1 \right] - I_{O2} \left[ \exp \left( \frac{q R_S I_{SC}}{a_2 k N_C T} \right) - 1 \right] - \frac{R_S I_{SC}}{R_P} \quad (16)$$

$$\begin{aligned} \text{Therefore, } I_{PV} &= I_{SC} + I_{O1} \left[ \exp \left( \frac{q R_S I_{SC}}{a_1 k N_C T} \right) - 1 \right] \\ &\quad + I_{O2} \left[ \exp \left( \frac{q R_S I_{SC}}{a_2 k N_C T} \right) - 1 \right] + \frac{R_S I_{SC}}{R_P} \end{aligned} \quad (17)$$

From Eqs. (15) and (17) we have;

$$I_{O2} = \frac{I_{SC} + \frac{R_S I_{SC}}{R_P} - \frac{V_{OC}}{R_P} - I_{O1} \left[ \exp \left( \frac{q V_{OC}}{a_1 k N_C T} \right) - \exp \left( \frac{q R_S I_{SC}}{a_1 k N_C T} \right) \right]}{\exp \left( \frac{q V_{OC}}{a_2 k N_C T} \right) - \exp \left( \frac{q R_S I_{SC}}{a_2 k N_C T} \right)} \quad (18)$$

Substituting Eq. (18) into Eq. (15) yields;

$$\begin{aligned} I_{PV} &= I_{O1} \left[ \exp \left( \frac{q R_S I_{SC}}{a_1 k N_C T} \right) - 1 \right] \\ &\quad + \frac{I_{SC} + \frac{R_S I_{SC}}{R_P} - \frac{V_{OC}}{R_P} - I_{O1} \left[ \exp \left( \frac{q V_{OC}}{a_1 k N_C T} \right) - \exp \left( \frac{q R_S I_{SC}}{a_1 k N_C T} \right) \right]}{\left[ \exp \left( \frac{q V_{OC}}{a_2 k N_C T} \right) - \exp \left( \frac{q R_S I_{SC}}{a_2 k N_C T} \right) \right] \left[ \exp \left( \frac{q V_{OC}}{a_2 k N_C T} \right) - 1 \right]^{-1}} + \frac{V_{OC}}{R_P} \end{aligned} \quad (19)$$

At the maximum power point,  $V = V_{MPP}$  and  $I = I_{MPP}$  (say); then, from Eq. (13) we obtain;

$$\begin{aligned} I_{MPP} &= I_{PV} - I_{O1} \left[ \exp \frac{q(V_{MPP} + R_S I_{MPP})}{a_1 k N_C T} - 1 \right] - I_{O2} \left[ \exp \frac{q(V_{MPP} + R_S I_{MPP})}{a_2 k N_C T} - 1 \right] \\ &\quad - \frac{V_{MPP} + R_S I_{MPP}}{R_P} \end{aligned} \quad (20)$$

## EQUILIBRIUM OPTIMIZER (EO) ALGORITHM

In this section, we discuss the exploratory and exploitative phases of EO, inspired by the general mass balance equation for a control volume (*Faramarzi et al., 2020*).

### Initialization and evaluation of functions

Like many metaheuristic algorithms, the EO uses the initial population for beginning the optimization process. The processing in this method is divided into two phases: the first phase is the “teacher phase,” which means learning from the teacher, and the second phase is the “learner phase,” which means learning by interacting with other learners.

These phases are consequently iterated to produce better results until convergence is achieved. In EO, each particle (solution) with its concentration (position) acts as a search agent. Some solutions and their dimensions experience mutation, defined by a function, and selected by a parameter such as mutation probability and percentage. The initial concentration is structured according to the particle number and dimensions, with normal initialization appearing as follows:

$$C_i^{initial} = C_{min} + rand_i(C_{max} - C_{min}) \quad i = 1, 2, \dots, n \quad (21)$$

$C_i^{initial}$  is the initial condensation of the  $i$ th particle,  $C_{max}$  and  $C_{min}$  are the maximum and minimum of the dimensions, respectively, and  $rand_i$  is in the domain  $[0, 1]$  so that  $n$  is the particle number representing a population. Particles are examined and thereafter classified as candidates.

### Equilibrium pool and candidates $C_{eq}$

The equilibrium case takes into consideration the last case of convergence of the algorithm, which should be the global optimum. At the beginning of the optimization algorithm, the equilibrium state is unknown, and it is only determined by the candidate that the equilibrium data creates a research model for particles. Depending on various factors, these candidates are identified, four particles specific to the optimization, and the condensation of others particle is the arithmetic mean of those. The number of candidates is random and depends on the nature of the problem. For example, the GWO uses the three best candidates ( $\beta$ ,  $\gamma$  and  $\alpha$  wolves) to change place with other wolves. More than four candidates can positively impact these five particles and are used as candidates for balancing to build a vector that is the equilibrium set in Eq. (22):

$$\vec{C}_{eq,pool} = \{\vec{C}_{eq(1)}, \vec{C}_{eq(2)}, \vec{C}_{eq(3)}, \vec{C}_{eq(ave)}\} \quad (22)$$

Every particle at every repetition changes its condensation to select randomly from the candidate's selection with the same prospect.

### Exponential term ( $F$ )

The following exponential expression ( $F$ ) contributes to the rule of changing condensation. A precise introduction of this expression leads to the balance of exploration and exploitation. The fluctuation range can change over time in an actual dominance volume, and should be a vector in the domain of  $[0, 1]$  as in Eq. (23):

$$\vec{F} = e^{-\vec{\lambda}(t-t_0)} \quad (23)$$

Thus, time,  $t$ , known as the task of iteration ( $Iter$ ), reduces the repetition number of Eq. (24):

$$t = \left(1 - \frac{Iter}{Max\_iter}\right)^{(a_2 \frac{Iter}{Max\_iter})} \quad (24)$$

where,  $Max\_iter$  and  $Iter$  represent the maximum number of iterations and the current,

respectively, and  $a_2$  is a constant utilized to administer the capacity of use. To warranty concourse and improve the exploration and exploitation capacity of the EO, this is given as;

$$\vec{t}_o = \frac{1}{\lambda} \ln(-a_1 \text{sign}(\vec{r} - 0.5)[1 - e^{-\lambda t}]) + t \quad (25)$$

Here,  $a_1$  is a constant that controls the exploration capacity, while  $a_2$  is a constant that controls the exploitation ability. Furthermore,  $r$  is a vector in the range [0–1] selected randomly.  $\text{Sign}(r - 0.5)$  impacts the direction of exploration and exploitation.  $a_1$  and  $a_2$  are two and one, respectively, for all problems. The derived form of Eq. (23) with the substitution Eq. (25) is represented in Eq. (26) as follows:

$$\vec{F} = a_1 \text{sign}(\vec{r} - 0.5)[e^{-\lambda t} - 1] \quad (26)$$

### Generation rate ( $G$ )

$G$  is another key expression of the proposed technique for providing the precise solution by enhancing exploitation. For example, a multipurpose model that characterizes  $G$  as the top-order exponential decomposition operation is as follows:

$$\vec{G} = \vec{G}_o e^{-K(t-t_o)} \quad (27)$$

where,  $G_o$  is the initial value and  $k$  represents the attenuation constant. For restricting the random variables, suppose that  $K = \lambda$ , and utilize the formerly derived exponential expression. The conclusive set of  $G$  is as follows:

$$\vec{G} = \vec{G}_o e^{-\lambda(t-t_o)} = \vec{G}_o \vec{F} \quad (28)$$

$$\text{where : } \vec{G}_o = \vec{G} \text{CP}(\vec{C}_{eq} - \vec{\lambda} \vec{C}) \quad (29)$$

$$\text{GCP} = \begin{cases} 0.5r_1 & r_2 < \text{GP} \\ 0 & r_2 \geq \text{GP} \end{cases} \quad (30)$$

Here,  $GCP$  is the control parameter for the generation rate that contains the potential of the generation expression assistance for the update procedure. In addition,  $r_1$  and  $r_2$  are random vectors in [0, 1]. Finally, the EO update rule is as in Eq. (31):

$$\vec{C} = \vec{C}_{eq} + (\vec{C} - \vec{C}_{eq}) \cdot \vec{F} + \frac{\vec{G}}{\lambda V} (1 - \vec{F}) \quad (31)$$

where,  $F$  is presented in Eq. (26), and  $V$  is a unit. To summarize all the aforementioned steps, a framework for EO is drawn in Fig. 4. It displays a conceptual sketch of the cooperation of all candidates for balance in a set of sample particles and how they sequentially affect the concentration update in the proposed algorithm. Since the topological positions of the equilibrium candidates are different in the initial iteration, and the exponential term generates large random numbers, this step-by-step update process helps particles that cover the entire area of the research. In the latter case, the opposite scenario occurs iterations when candidates circle the sweet spot with similar attitudes.

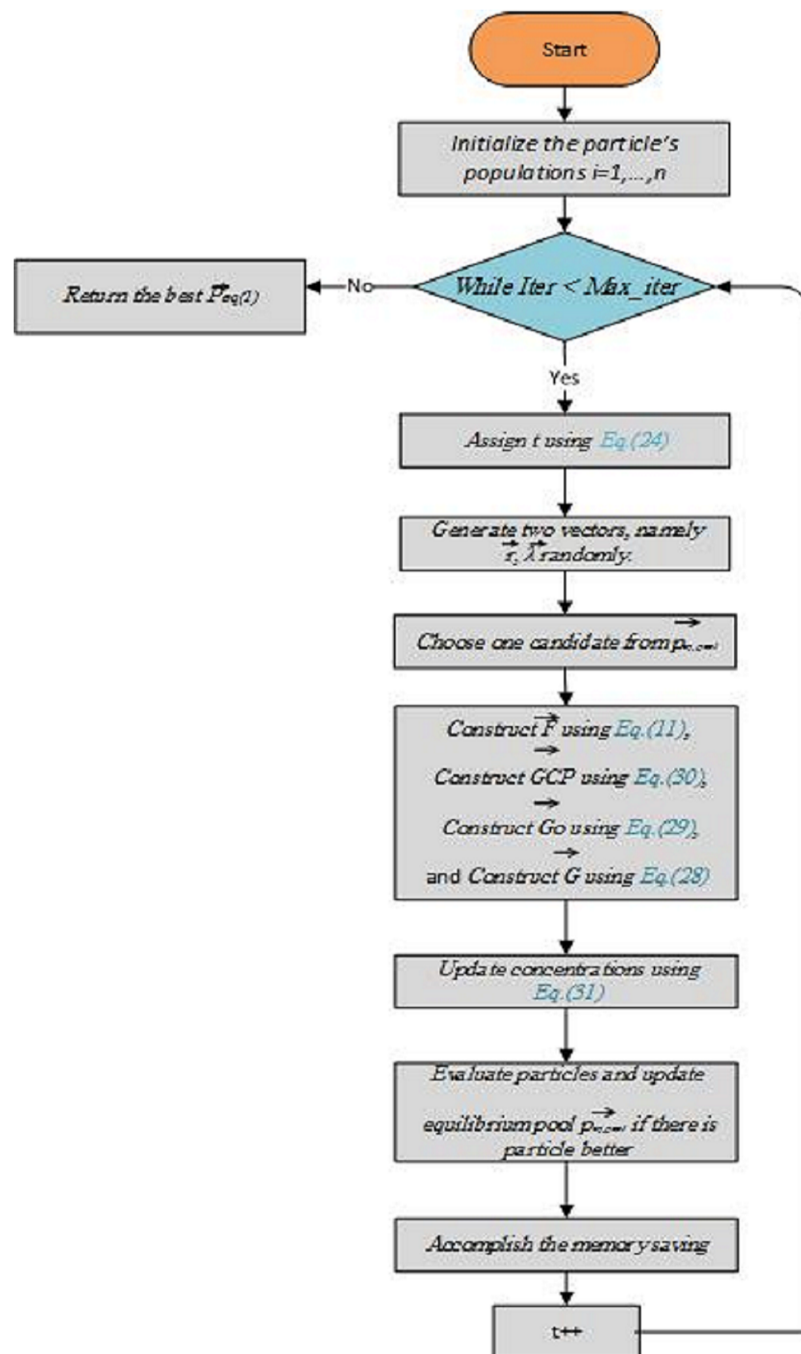


Figure 4 A flowchart of the equilibrium optimizer (EO) algorithm.

Full-size DOI: 10.7717/peerj-cs.708/fig-4

To this sometimes the exponential term generates small random numbers, which helps in refining the solutions. Providing smaller step sizes. This concept can also be extended to higher dimensions such as hyperspace in which the concentration is updated with the movement of the particle in  $n$ -dimensional space.

The EO algorithm has been tested for three known engineering design problems. A simple method of constraint management, the static penalty, is used here to punish the objective function with high score when constraints are violated at any level from their defined limits. The penalty coefficient must be large enough to correctly punish the objective function under the conditions of equality/inequality. Note that all technical test problems ran with the same number of iterations (500) and particles (30) according to the math functions described above.

## IMPROVED EQUILIBRIUM OPTIMIZER (IEO) ALGORITHM

We improved the Equilibrium Optimizer algorithm to give the best result that is closest to the global optimum. The improvement has been done by using opposition-based learning (OBL). The Equilibrium Optimizer algorithm with OBL gave better values to the unknown parameters of PV than Equilibrium optimizer without improvement.

### Opposition based learning (OBL)

The basic concept of Opposition-Based Learning (OBL) was originally introduced by [Tizhoosh \(2005\)](#). The basic aim of this algorithm is optimization, to find the best candidate solution, the simultaneous consideration of an estimate and its corresponding opposite estimate which is closer to the global optimum. This has been achieved in a very short time and it has been used in various areas of soft computing. Opposition-based Learning (OBL), which has been used for improving convergence of the metaheuristic techniques for finding the global solution of the optimization problem. OBL theory has been applied to solve many real-world problems such as optimization and estimation of photovoltaic parameters. In general, any metaheuristic algorithm begins with creating an initial population as an attempt for finding the optimum solution(s), these initial solutions are generated randomly or based on a specific search range.

#### Opposite number

$x$  is defined as a real number over the domain  $x \in [lb, ub]$ . The opposite of  $x$  is represented by  $\bar{x}$  and to identified as:

$$\bar{x} = ub + lb - x \quad (32)$$

where  $ub$  and  $lb$  are the upper and lower bound of the search space. Eq. (32) can be generalized to be used in a search area with multi-dimensions. Therefore, to generalize it, every search-agent position and its opposite position will be introduced as the following:

$x = [x_1, x_2, x_3, x_4, \dots, x_D]$  and  $\bar{x} = [\bar{x}_1, \bar{x}_2, \bar{x}_3, \bar{x}_4, \dots, \bar{x}_D]$  The values of all parameters in  $\bar{x}$  will be estimated as:

$$\bar{x}_j = ub_j + lb_j - x_j \quad \text{where } j = 1, 2, 3, \dots, D \quad (33)$$

#### Opposition based learning

In this optimization strategy if the fitness function  $f(x)$  of its original solution, then  $x = \bar{x}$ ; otherwise  $x = x$ .

**Table 2** Optimized parameters for the single-diode and double-diode model.

Models	Optimized variables	Calculated variables
Single-diode model	a, Rs, Rp	$I_o$ (Eq. (9)) and $I_{PV}$ (Eq. (10))
Double-diode model	a1, a2, Rs, Rp, $I_{o1}$	$I_{o2}$ (Eq. (18)) and $I_{PV}$ (Eq. (19))

## OBJECTIVE FUNCTION

The major purpose of estimating the parameters for SDM and DDM is to detect the parameter values that reduce the differences between the measured and calculated current that can be determined with an objective function. **Table 2** presents details about the parameters that are optimized by IEO technique. The parameters were computed depending on the special connections that were discussed in ‘Mathematical Model of Photovoltaic Cell/Module’ for the SDM and DDM. For the DDM,  $(a_1)$ ,  $(a_2)$ ,  $(R_S)$ ,  $(R_P)$  and  $(I_{o1})$  are optimized  $(I_{PV})$  and  $(I_{o2})$  are computed by variables that are optimized utilizing the relationship discussed in ‘Mathematical Model of Photovoltaic Cell/Module’. Metaheuristic algorithms are necessary to minimize errors at three points (open circuit  $[0, V_{OC}]$ , short circuit  $[I_{SC}, 0]$ , and points of maximum power  $[I_{MPP}, V_{MPP}]$ ). For the SDM, the error at the open circuit (from Eq. (6)) is;

$$err_{OC} = I_O \left[ \exp\left(\frac{qV_{OC}}{akN_C T}\right) - 1 \right] + \frac{V_{OC}}{R_p} - I_{PV} \quad (34)$$

The error at the short circuit (from Eq. (8)) is;

$$err_{SC} = I_{SC} + I_O \left[ \exp\left(\frac{qR_S I_{SC}}{akN_C T}\right) - 1 \right] + \frac{R_S I_{SC}}{R_p} - I_{PV} \quad (35)$$

The error at the maximum power point (from Eq. (11)) is;

$$err_{MPP} = I_{PV} - I_O \left[ \exp\left(\frac{q(V_{MPP} + R_S I_{MPP})}{akN_C T}\right) - 1 \right] - \frac{V_{MPP} + R_S I_{MPP}}{R_p} - I_{MPP} \quad (36)$$

The same applies for the error values of the DDM, which can be derived using Eqs. (15), (17) and (20) at these three points. The goal of optimization is considered the sum of the quadratic errors:

$$ERR = err_{OC}^2 + err_{SC}^2 + err_{MPP}^2 \quad (37)$$

## SIMULATION RESULTS AND ANALYSIS

To verify the accuracy, reliability, and robustness of the IEO algorithm, we evaluate the performance of the IEO algorithm for estimating the parameters of a PV cell, namely, the SDM and DDM. For every SDM and DDM for all SC types (polycrystalline, thin-film, and monocrystalline), the IEO were run separately 30 times. A MATLAB model was developed for testing the algorithms presented above. In addition, variables such as open-circuit voltage ( $V_{OC}$ ), short circuit current ( $I_{SC}$ ), maximum power point voltage

**Table 3** Electrical variables for photovoltaic (PV) cell under the standard test conditions.

Variables	Kyocera KC200G	Shell SQ85	Shell ST40
Kind	Polycrystalline	Monocrystalline	Thin film
Open circuit voltage, $V_{oc}$ (volt)	32.9	22.2	23.3
Short circuit current, $I_{sc}$ (amp)	8.21	5.45	2.68
Voltage at maximum power, $V_{MPP}$ (volt)	26.3	16.6	17.2
Current at maximum power, $I_{MPP}$ (amp)	7.61	4.95	2.41
Temperature coefficient of $V_{oc}$ , $K_{V,OC}$	-0.123	-0.0725	-0.1 ( $\text{volt}/^{\circ}\text{C}$ )
Temperature coefficient of $I_{SC}$ , $K_{I,SC}$	$3.18 \times 10^{-10}$	$0.8 \times 10^{-10}$	$0.35 \times 10^{-10}$ ( $\text{volt}/^{\circ}\text{C}$ )
Number of cells in series, $N_C$	54	36	36

**Table 4** Input variables to the Improved Equilibrium Optimizer (IEO) algorithm.

Parameters	SDM	DDM
Dimension of problem $d$	3	5
Initial population size, $N_{pini}$	50	80
Maximum no. of fitness evaluation, $NFE_{max}$	50	60
The range of parameters, $[X_{min}, X_{max}]$	$a = [0.1, 2.0]$	$a_1 = [0.1, 2.0]$ $a_2 = [0.1, 2.0]$
	$R_s = [0.0001, 1] \text{ ohm}$	$I_{o1} = [10^{-12}, 10^{-06}] \text{ amp}$
	$R_p = [40; 200] \text{ ohm}$	$R_s = [0.0001, 1] \text{ ohm}$ $R_p = [40, 200] \text{ ohm}$

( $V_{MP}$ ), maximum power point current ( $I_{MP}$ ), voltage temperature coefficient ( $K_V$ ), and current temperature coefficient ( $K_i$ ) were provided in the manufacturer's data sheet. All characteristics passed through three specified points are illustrated in **Table 3** as follows: Open circuit:  $V = V_{OC} = 32.9$  volt,  $I = 0$  amp; Short circuit:  $V = 0$  volt,  $I = I_{SC} = 8.21$  amp; Maximum power:  $V = V_{MPP} = 26.3$  volt,  $I = I_{MPP} = 7.61$  amp. The algorithm was run on the MATLAB R2010a platform on a system with 4 GB RAM and an i3 processor. Improved code of equilibrium optimization using opposition-based learning is available in supplemental [Source\\_Code](#) file. Code to generated datasets used to test the code is available inside supplemental [Datasets File](#). After improved Equilibrium optimization by opposition-based learning, we found the algorithm found best error than before.

## Numerical data

This study examined three types of SCs: polycrystalline, thin-film, and monocrystalline. Exemplary data supplied by the industries are displayed in **Table 3**. This table illustrates which current and voltage data at the three main points are explicitly specified at standard test conditions, such as irradiance of 1,000 w/m<sup>2</sup> and temperature of 25 °C. Additional details of the parameters measured by the aforementioned equations are listed in **Table 4**.

**Table 5** Optimal variables estimated by the IEO for the single-diode model of polycrystalline, Kyocera KC200GT.

Run-No	Optimized parameters			Calculated parameters		Error
	$a$	$R_S$ (ohm)	$R_P$ (ohm)	$I_O$ (amp)	$I_{PV}$ (amp)	
1	0.4105	0.0007	43.839	3.07E-27	8.2101	0
2	0.3494	0.001	43.835	5.06E-32	8.2102	0
3	1.0464	0.001	50.5571	1.37E-10	8.2102	1.39E-28
4	1.1205	0.001	53.4895	7.05E-10	8.2102	9.66E-26
5	0.3712	0.0008	43.8341	3.91E-30	8.2102	0
6	1.3315	0.0449	78.0334	2.81E-08	8.2147	6.53E-27
7	1.6246	0.001	151.2808	9.62E-07	8.2101	0
8	0.4774	0.001	43.8344	2.13E-23	8.2102	0
9	1.3325	0.0089	70.3248	2.84E-08	8.211	3.94E-30
10	0.3517	0.2152	43.6181	8.21E-32	8.2505	0
11	1.0185	0.0002	49.6954	6.93E-11	8.21	0
12	0.416	0.0753	43.7651	7.13E-27	8.2241	0
13	0.9492	0.001	43.8343	1.07E-11	8.2102	0
14	1.2509	0.1403	95.3509	8.12E-09	8.2221	7.59E-25
15	0.5229	0.0104	43.8229	2.37E-21	8.2119	0
16	1.447	0.1103	181.9726	1.37E-07	8.2149	0
17	0.4153	0.0374	43.7961	6.38E-27	8.217	0
18	0.4778	0.0004	43.8338	2.22E-23	8.2101	3.16E-30
19	0.9559	0.0007	43.8341	1.30E-11	8.2101	1.58E-25
20	0.7702	0.001	44.991	1.89E-14	8.2102	7.61E-28
21	1.6672	0.0009	190.3722	1.45E-06	8.21	0
22	1.6277	0.0009	153.5346	9.93E-07	8.2101	2.84E-29
23	1.675	0.001	200	1.56E-06	8.21	2.23E-25
24	1.1749	0.2297	135.4552	2.16E-09	8.2239	0
25	0.9312	0.0498	43.7842	6.33E-12	8.2193	7.88E-31
26	0.8439	0.0009	45.863	3.58E-13	8.2102	0
27	0.9436	0.0013	47.7275	9.17E-12	8.2102	0
28	1.6677	0.0008	193.4348	1.46E-06	8.21	0
29	0.4168	0.1344	43.7342	7.98E-27	8.2352	0
30	1.266	0.0709	74.3245	1.03E-08	8.2178	0

## Results of the single diode model

Every group of the optimal variables was estimated by several runs led to zero error at the three main I-V points. There were three types of SCs: Polycrystalline cell Kyocera KC200GT, monocrystalline cell Shell SQ85, and thin film ST40. The run of each type is presented in this subsection. **Table 5** presents the optimal parameters of the SDM for the polycrystalline cell Kyocera KC200GT using the IEO. **Table 5** also presents the accuracy of the IEO in generating the PV parameters. The results of the best run of the

**Table 6** Optimal variables estimated by the IEO for the single-diode model of monocrystalline photovoltaic cell, Shell SQ85.

Run-No	Optimized parameters			Calculated parameters		Error
	$a$	$R_S$ (ohm)	$R_P$ (ohm)	$I_O$ (amp)	$I_{PV}$ (amp)	
1	0.4952	0.001	42.4047	5.19E-23	5.1979	0
2	1.9999	0.0248	142.2184	1.08E-05	5.3762	0
3	1.9975	0.0478	179.6755	1.07E-05	5.3926	0
4	2	0.0381	162.6624	1.09E-05	5.3861	0
5	2.0000 0	0.0546	200	1.09E-05	5.3987	0
6	2	0.0009	115.7362	1.08E-05	5.3576	$67.88E-31$
7	1.1357	0.0031	45.5716	4.76E-10	5.2158	0
8	1.9955	0.001	113.9509	1.04E-05	5.3562	0
9	2	0.001	115.7355	1.07E-05	5.3576	0
10	0.5286	0.151	41.3043	1.48E-21	5.2209	0
11	1.9986	0.001	115.1735	1.07E-05	5.3572	$1.55E-28$
12	0.322	0.001	42.401	2.26E-35	5.1978	0
13	2	0.001	115.7355	1.08E-05	5.3576	0
14	2	0.0009	115.7381	1.08E-05	5.3576	0
15	1.6533	0.2203	200	7.02E-07	5.4055	0
16	2	0.0009	115.7466	1.08E-05	5.3576	0
17	0.2549	0.1756	40.2245	1.12E-44	5.2198	0
18	2	0.0546	200	1.09E-05	5.3987	0
19	2	0.001	115.7355	1.08E-05	5.3576	0
20	1.9986	0.001	115.1901	1.07E-05	5.3572	0
21	1.9999	0.0546	199.8438	1.09E-05	5.3987	0
22	0.3164	0.0514	41.3486	5.44E-36	5.2014	$1.16E-26$
23	2	0.0009	115.7405	1.08E-05	5.3576	0
24	1.6864	0.001	58.2724	9.08E-07	5.2665	0
25	0.4776	0.182	40.2556	7.38E-24	5.2213	0
26	1.9928	0.001	112.8824	1.03E-05	5.3553	0
27	1.8995	0.0389	107.3014	5.37E-06	5.3533	0
28	0.2306	0.001	40.401	2.23E-49	5.1854	0
29	2	0.001	115.7355	1.08E-05	5.3576	0
30	0.8333	0.0478	41.0522	1.09E-13	5.1989	0

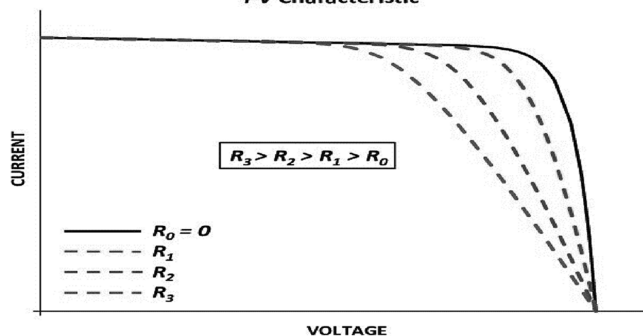
monocrystalline PV cell (Shell SQ85) are presented in Table 6. Table 7 presents the results obtained by the run of the thin-film PV cell (Shell ST40) using the IEO.

Tables 5–7 reveal a small difference in the values of series resistance  $R_S$  for both multicrystalline and monocrystalline. The I–V curve is strongly affected by the series resistance. According to the results, lower values of  $R_S$  lead the I–V characteristics to move farther from the axis with respect to the maximum point, while higher values of  $R_S$  lead the I–V characteristics to move closer to the axis as in Fig. 5. This tendency occurs naturally with the IEO parameter values.

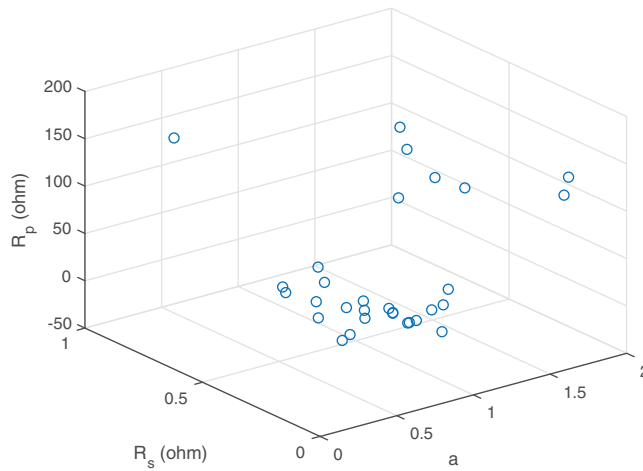
**Table 7** Optimal variables for the single-diode model of thin-film photovoltaic cell, Shell ST40.

Run-No	Optimized parameters			Calculated parameters		Error
	$a$	$R_S$ (ohm)	$R_P$ (ohm)	$I_O$ (amp)	$I_{PV}$ (amp)	
1	0.3722	0.0009	61.4825	1.90E-32	2.6800	0
2	2.0000	0.0055	80.7240	2.56E-06	2.6802	0
3	0.4832	0.1381	61.3438	4.47E-25	2.6860	0
4	1.8316	0.3748	86.4215	7.32E-07	2.6916	1.97E-31
5	2.0000	0.7718	200.00	2.75E-06	2.6910	0
6	2.0000	0.0010	80.5100	2.56E-06	2.6800	0
7	0.6324	1.0000	60.8257	3.06E-19	2.7241	0
8	2.0000	0.7718	200.00	2.75E-06	2.6903	0
9	0.2588	0.2059	61.2756	1.69E-46	2.6890	0
10	0.1561	0.6689	60.8125	7.74E-77	2.7095	0
11	2.0000	0.0085	80.8260	2.56E-06	2.6803	0
12	1.0287	0.3286	62.2278	5.72E-12	2.6942	0
13	1.9993	0.1227	85.1764	2.56E-06	2.6839	0
14	0.1848	0.8890	60.5925	5.42E-65	2.7193	1.51E-24
15	2.0000	0.6067	135.2353	2.69E-06	2.6920	0
16	1.0079	0.0010	61.8808	3.27E-12	2.6800	0
17	2.0000	0.5032	116.1444	2.66E-06	2.6916	0
18	2.0000	0.3980	103.5123	2.64E-06	2.6903	7.88E-31
19	2.0000	0.0010	80.5112	2.56E-06	2.6800	0
20	2.0000	0.7127	168.6513	2.73E-06	2.6913	1.37E-24
21	2.0000	0.4524	109.4282	2.65E-06	2.6911	0
22	2.0000	0.0009	80.5115	2.56E-06	2.6800	0
23	0.4069	0.0009	61.4825	1.03E-29	2.6800	0
24	0.1303	0.5279	60.9536	5.18E-92	2.7032	0
25	0.6593	0.5741	60.9933	1.79E-18	2.7052	8.27E-25
26	0.4683	0.0021	61.4795	7.28E-26	2.6801	4.43E-29
27	0.2947	0.3023	61.1791	6.99E-41	2.6932	0
28	0.9640	0.0308	61.7630	9.44E-13	2.6813	1.50E-26
29	0.2048	0.5737	60.9078	1.14E-58	2.7052	0
30	0.4355	0.5503	60.9320	8.85E-28	2.7042	0

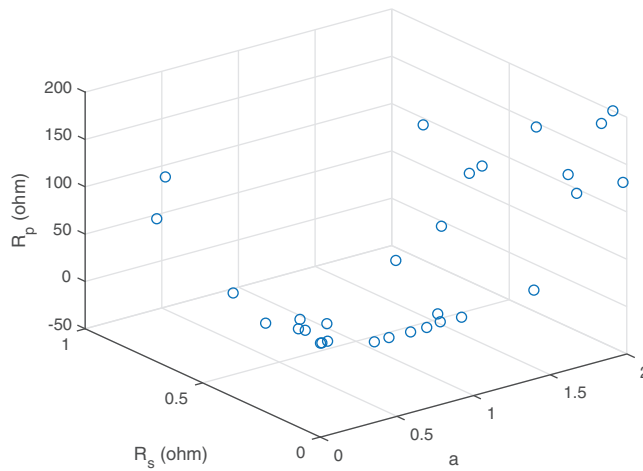
The difference between I-V characteristics can be attributed not only to different values of  $R_S$  and  $R_P$ , but also to ideality factor of the diode,  $a$ . It is demonstrated that the values of all variables change significantly. However, every optimal solution can arrive at zero error for the three major points. All prior studies displayed one I-V characteristic that passed across the three main points. However, a PV cell characteristic was observed that is not normal when the designer concentrated on the three major points. For each cell, there is an operating point on the characteristic in which the performance is greatest. These points are referred as the major points. The algorithm arrived at the global optimal

**I-V Characteristic****Figure 5 Effects of the series resistance on the I-Vcharacteristic.**

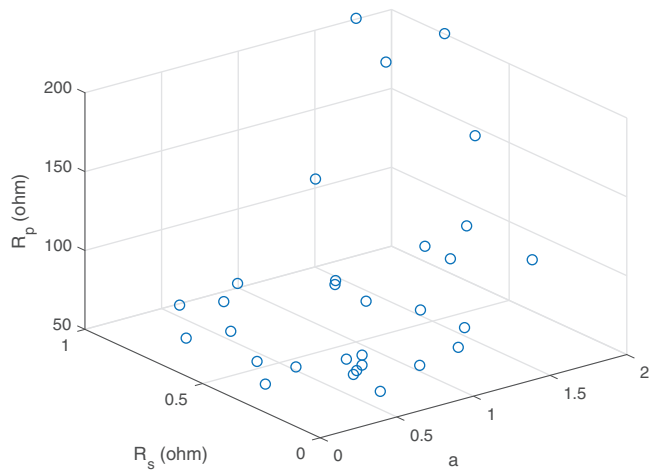
Full-size DOI: 10.7717/peerj-cs.708/fig-5

**Figure 6 Scatter plot of the optimalvalues (30 sets) for the single-diode model ofpolycrystalline cell KC200GT.**

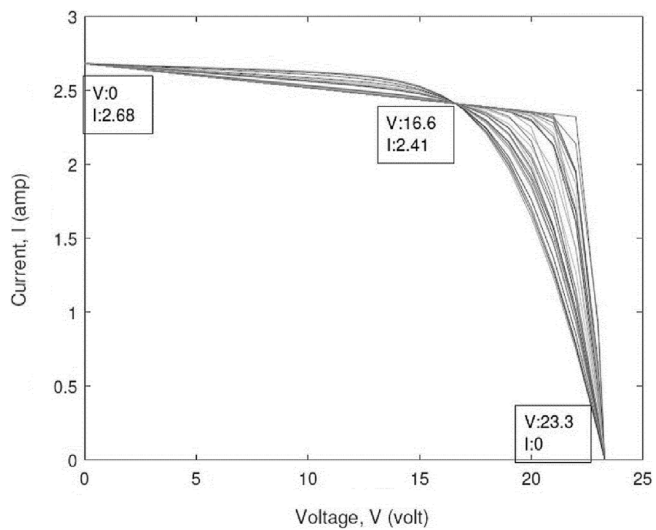
Full-size DOI: 10.7717/peerj-cs.708/fig-6

**Figure 7 Scatter plot of the optimalvalues for the single-diode model ofmonocrystalline cell SQ85.**

Full-size DOI: 10.7717/peerj-cs.708/fig-7

**Figure 8** Scatter plot of the optimalvalues for the single-diode model of thin-filmcell ST40.

Full-size DOI: 10.7717/peerj-cs.708/fig-8

**Figure 9** Plot of the optimal solutions for the single-diode model of thin-film cell ST40.

Full-size DOI: 10.7717/peerj-cs.708/fig-9

solution after 0.10 s with an error of zero value. This algorithm took less time to run compared to other metaheuristic algorithms.

A scatter plot of the optimal values (30 points) of these three parameters is provided in Figs. 6–8. It is showing that the value of each parameter changes significantly. This demonstrates that under the same parameter values  $I_{PV}$ ,  $I_O$ ,  $a$ ,  $R_S$  and  $R_P$ , the IEO algorithm has the highest efficiency for the experimental I-V data for every module.

As displayed in the previous figures, every curve passes through the three known points. A plot of the optimal solution is presented in Fig. 9. A difference in ( $a$ ) is present approximately between 0.2 and 1.7, while that of ( $R_p$ ) is approximately between 80 and 175 ohms.

**Table 8** Optimal variables for the double-diode model of polycrystalline photovoltaic cell, Kyocera KC200GT.

Run-No	Optimized parameters					Calculated parameters		Error
	$a_1$	$a_2$	$R_S$ (ohm)	$R_P$ (ohm)	$I_{O1}$ (amp)	$I_{O2}$ (amp)	$I_{PV}$ (amp)	
1	2.0000	1.5233	0.14386	67.3361	1.16E-07	3.21E-07	8.2275	0
2	1.8289	1.4930	0.2968	199.7722	1.00E-12	2.38E-07	8.2222	1.02E-29
3	2.0000	1.9995	0.0158	131.1378	1.00E-06	1.80E-05	8.2109	0
4	1.9915	1.2460	0.2805	61.5366	1.00E-12	7.34E-09	8.2474	0
5	1.9999	2.0000	0.0010	117.3639	1.00E-06	1.79E-05	8.2101	0
6	1.8059	1.5498	0.0010	50.0000	2.15E-07	4.013E-07	8.2102	0
7	1.9687	1.6440	0.0010	55.3115	1.00E-12	1.11E-06	8.2101	0
8	1.6413	2.0000	0.0012	117.0978	6.92E-09	1.89E-05	8.2101	0
9	2.0000	1.4957	0.0412	50.0000	1.00E-12	2.31E-07	8.2168	0
10	1.9717	1.9995	0.0010	117.1425	3.52E-09	1.89E-05	8.2101	0
11	2.0000	0.9102	0.4325	53.7084	4.62E-07	3.34E-12	8.2761	1.26E-29
12	1.6973	1.1087	0.2937	50.0000	2.34E-09	5.51E-10	8.2582	0
13	1.9769	2.0000	0.0027	118.7968	1.51E-12	1.90E-05	8.2102	0
14	2.0000	1.0519	0.3943	61.4608	1.00E-12	1.59E-10	8.2627	7.61E-28
15	1.8233	1.5153	0.0049	50.0000	1.00E-06	2.32E-07	8.2108	0
16	1.9087	1.5505	0.0010	50.0000	2.73E-07	4.13E-07	8.2102	7.89E-31
17	1.5751	2.0000	0.0141	129.5679	1.00E-12	1.91E-05	8.2109	0
18	1.9727	1.2646	0.1699	50.0000	1.00E-06	9.14E-09	8.2379	0
19	2.0000	2.0000	0.0012	117.5239	9.77E-07	1.80E-05	8.2101	0
20	1.9745	1.9999	0.0327	153.4717	1.00E-12	1.91E-05	8.2117	0
21	1.9170	2.0000	0.0010	117.3639	1.00E-12	1.89E-05	8.2101	7.13E-28
22	1.9999	1.5504	0.0012	50.0009	3.68E-07	4.15E-07	8.2102	0
23	1.9920	2.0000	0.0010	117.3640	1.00E-12	1.89E-05	8.2101	0
24	1.6250	1.4812	0.2960	200.0000	1.90E-07	1.67E-07	8.2222	0
25	1.5044	1.3441	0.1288	50.5678	9.34E-08	2.08E-08	8.2309	0
26	1.3900	1.9999	0.0010	117.3636	1.00E-12	1.89E-05	8.2101	0
27	1.9999	2.0000	0.0010	117.3639	7.48E-09	1.89E-05	8.2101	0
28	2.0000	1.9947	0.0320	148.5751	2.98E-09	1.85E-05	8.2118	0
29	1.9904	1.5530	0.0034	50.0000	1.39E-08	4.36E-07	8.2106	3.15E-30
30	1.9982	0.5695	0.6635	55.6877	1.53E-09	1.41E-19	8.3078	7.88E-31

## Results of the double diode model

Using the (same parameter values)  $I_{ph}$ ,  $I_{o1}$ ,  $I_{o2}$ ,  $a_1$ ,  $a_2$ ,  $R_S$ , and  $R_P$ , IEO is more consistent with the experimental I-V data of all types of modules. The estimation of the parameters of SCs based on the DDM has high precision, and the optimization of parameters is implemented for the DDM of different types. A total of five parameters are optimized for the DDM ( $a_1$ ,  $a_2$ ,  $R_S$ ,  $R_P$ ,  $I_{O1}$ ), while two sustainable parameters are calculated ( $I_{O2}$ ,  $I_{PV}$ ) for their relation with the optimized parameters. The optimized parameters in various runs of the IEO algorithm for the DDM polycrystalline, KC200GT cell are listed in

**Table 9** Optimal variables for the double-diode model of monocrystalline Shell SQ85.

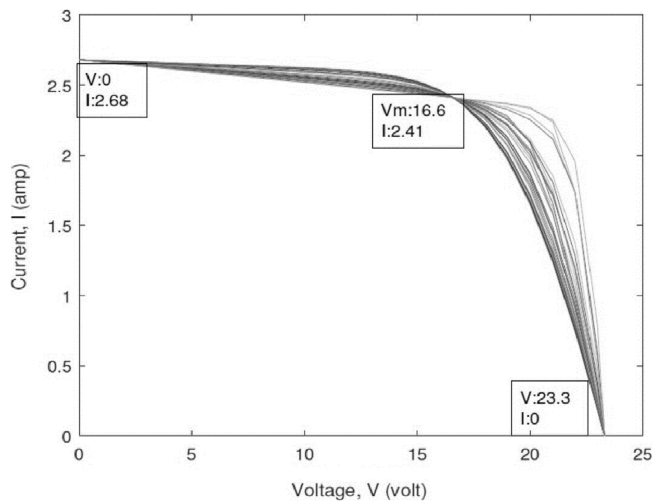
Run-No	Optimized parameters					Calculated parameters		Error
	$a_1$	$a_2$	$R_S$ (ohm)	$R_P$ (ohm)	$I_{O1}$ (amp)	$I_{O2}$ (amp)	$I_{PV}$ (amp)	
1	2.0000	1.3534	0.1210	50.0000	7.84E-07	1.82E-08	5.4632	0
2	2.0000	2.0000	0.0010	117.3655	1.00E-12	1.08E-05	5.4500	0
3	2.0000	1.5570	0.0010	50.0000	1.00E-12	2.47E-07	5.4501	0
4	2.0000	1.7412	0.0261	69.0104	4.49E-07	1.43E-06	5.4521	0
5	1.9727	2.0000	0.0010	117.0170	8.39E-07	9.76E-06	5.4500	0
6	1.9675	2.0000	0.0010	117.3639	1.00E-12	1.08E-05	5.4500	7.88E-31
7	2.0000	1.5394	0.0010	50.0000	1.00E-06	1.84E-07	5.4501	0
8	1.8821	2.0000	0.0010	114.3371	9.90E-07	8.51E-06	5.4500	0
9	1.7597	1.9999	0.0056	119.4022	1.22E-07	1.00E-05	5.4503	0
10	1.7776	0.6201	0.5195	50.0000	5.62E-07	1.64E-18	5.5066	3.16E-28
11	1.9716	1.8592	0.0010	80.0694	1.00E-06	3.48E-06	5.4501	0
12	1.5348	1.5560	0.0016	50.0000	1.05E-12	2.44E-07	5.4502	0
13	1.9755	1.2397	0.2009	50.0005	3.33E-07	3.21E-09	5.4719	0
14	1.9170	2.0000	0.0010	117.3642	1.00E-12	1.08E-05	5.4500	0
15	1.8099	1.2020	0.4245	158.2137	1.00E-12	1.82E-09	5.4646	0
16	1.5581	1.5565	0.0010	50.0000	3.09E-07	5.85E-08	5.4501	0
17	1.9975	0.5000	0.6887	50.0000	1.00E-12	8.92E-23	5.5251	0
18	1.7492	2.0000	0.0010	117.3639	1.00E-12	1.08E-05	5.4500	6.19E-25
19	1.9707	2.000	0.00013	117.5777	1.00E-12	1.08E-05	5.4501	0
20	1.9769	2.0000	0.0237	140.7349	1.33E-07	1.07E-05	5.4509	0
21	1.8546	1.6003	0.2212	145.2258	2.37E-07	3.87E-07	5.4583	7.88E-31
22	1.8666	1.2806	0.2578	66.6718	8.05E-07	5.39E-09	5.4711	0
23	1.7608	1.9859	0.0023	112.7487	1.00E-12	9.80E-06	5.4501	0
24	2.0000	2.0000	0.0010	117.3639	3.79E-07	1.04E-05	5.4500	0
25	2.0000	2.0000	0.0546	200.0000	1.00E-06	9.93E-06	5.4515	1.97E-29
26	1.9668	1.9200	0.0095	96.2587	5.21E-07	5.82E-06	5.4505	0
27	1.8934	2.0000	0.0037	119.6661	3.89E-09	1.08E-05	5.4502	0
28	1.9697	1.9996	0.0010	116.9501	5.45E-07	1.01E-05	5.4500	4.65E-25
29	2.0000	2.0000	0.0010	117.3639	1.03E-12	1.08E-05	5.4500	0
30	1.9478	1.5355	0.0010	50.0000	1.00E-06	1.68E-07	5.4501	0

**Table 8**, SQ85 monocrystalline dish are listed in **Table 9** and thin cells, shell ST40 are displayed in **Table 10**. For the SDM, the optimized parameters resulted in zero error at the three main points. The 30 I-V characteristics resulting from various combinations of the variables are presented in **Fig. 9**. A plot of the optimal solution is presented in **Fig. 10**. All the curves passed through the open circuit, short circuit, and maximum power points. To easily analyze the optimized variables, standardized parameter values are presented in a parallel coordinate graph in **Fig. 11**. The value of  $R_P$  differs widely. However,  $I_{O1}$  ranges from approximately 0.01 to 0.9p.u. The final value of the diode saturation current is very low, with an average of only  $\mu A$

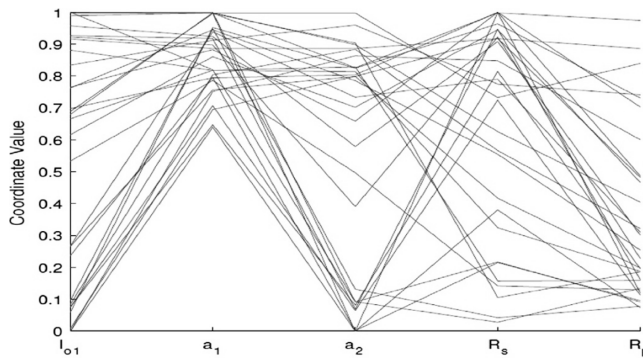
**Table 10** Optimal variables for the double-diode model of thin-film photovoltaic cell, Shell ST40.

Run-No	Optimized parameters					Calculated parameters		Error
	$a_1$	$a_2$	$R_S$ (ohm)	$R_P$ (ohm)	$I_{OI}$ (amp)	$I_{O2}$ (amp)	$I_{PV}$ (amp)	
1	1.9497	0.8051	0.0010	61.5456	1.00E-12	3.39E-15	2.6800	0
2	2.0000	1.9998	0.7719	199.9620	1.00E-06	1.75E-06	2.6904	7.96E-29
3	2.0000	0.6828	0.1757	61.7124	1.68E-07	6.97E-18	2.6876	0
4	2.0000	1.7425	1.0000	200.0000	1.00E-06	2.30E-07	2.6934	0
5	1.9999	0.8567	0.0518	61.5676	3.69E-09	2.65E-14	2.6823	0
6	1.9495	2.0000	0.2125	89.6850	1.00E-12	2.59E-06	2.6864	0
7	1.7032	0.5000	0.4038	64.0517	1.79E-07	6.46E-25	2.6969	0
8	1.6443	1.5964	0.4139	75.9185	2.32E-07	6.12E-08	2.6946	1.84E-25
9	1.9999	0.5185	0.0010	63.3347	1.00E-06	1.28E-23	2.6800	0
10	1.9396	2.0000	0.7815	199.6071	1.00E-06	1.22E-06	2.6905	1.77E-30
11	2.0000	0.5958	0.5694	63.31576	6.10E-07	1.60E-20	2.7041	4.20E-27
12	1.8235	0.5501	1.0000	60.5959	1.00E-12	4.59E-22	2.7242	0
13	1.9419	0.5000	0.8368	60.6656	1.00E-12	3.05E-24	2.7169	0
14	1.9999	0.5000	0.0010	63.3348	1.00E-06	1.80E-24	2.6800	0
15	1.7237	0.5000	0.7316	60.7619	1.00E-12	3.05E-24	2.7123	0
16	1.7183	0.6149	1.0000	62.3562	4.42E-08	7.48E-20	2.7229	0
17	1.7775	2.0000	0.8158	200.0000	3.65E-07	7.10E-07	2.6909	3.86E-29
18	1.8125	1.6049	0.9979	132.9710	3.09E-07	4.81E-08	2.7001	0
19	1.4287	0.5322	0.7106	71.8892	4.00E-08	2.46E-22	2.7065	1.13E-28
20	1.9741	0.5007	0.0049	62.6031	5.44E-07	2.40E-24	2.6802	0
21	1.9138	1.9787	0.7749	188.6456	1.21E-09	2.37E-06	2.6910	1.77E-30
22	2.0000	0.5000	0.2572	61.2253	1.00E-12	3.02E-24	2.6913	0
23	1.9783	0.7001	0.0021	61.4963	1.01E-12	2.02E-17	2.6801	0
24	2.0000	0.5000	1.0000	60.5306	1.00E-12	3.06E-24	2.7242	0
25	1.9991	0.5000	0.4302	61.0538	1.00E-12	3.03E-24	2.6989	0
26	1.4757	0.7693	0.0010	61.5234	1.06E-12	6.90E-16	2.6800	0
27	1.9429	1.3129	0.6557	71.6179	3.02E-07	1.57E-09	2.7045	0
28	1.9632	2.0000	0.0010	80.3427	8.82E-07	1.42E-06	2.6800	0
29	2.0000	0.5000	0.1255	62.7184	6.31E-07	2.26E-24	2.6854	0
30	1.7438	0.5000	0.1682	63.5249	2.48E-07	7.51E-25	2.6871	0

To summarize, regardless of the type of the PV cell or the PV parameter extraction model used, we cannot obtain one I-V characteristic with details of short circuits, maximum power, and open circuit points. A total of three point optimizations can reveal various characteristics in several tests. ‘Simulation Results and Analysis’ confirms the effectiveness of the IEO algorithm in estimating the parameters of the SC, taking into account the SDM and DDM. In addition, the SDM used three types of PV modules to estimate the parameters of the PV model.

**Figure 10** Plot of the optimal solutions for the double-diode model of thin film ST40.

Full-size DOI: 10.7717/peerj-cs.708/fig-10

**Figure 11** Parallel coordinate plot of the optimal solutions for the double-diode model of thin-film ST40.

Full-size DOI: 10.7717/peerj-cs.708/fig-11

## RESULTS OF COMPARING THE EFFECIENCY OF THE IEO WITH OTHER METAHEURISTIC ALGORITHMS

The results of SC parameter estimation are compared with the results of other metaheuristic algorithms to evaluate the efficiency of applying the IEO algorithm.

### The single diode model

This subsection presents a comparison between the solutions generated by the IEO algorithm and other algorithms that have been applied under the same conditions. The optimal error values obtained by the IEO was zero, as presented in [Table 11](#). The IEO achieves the best results among all the six algorithms tested, followed by SCA, while the GA achieves the poorest results.

### The double diode model

This subsection provides a comparison between the solutions generated by the IEO algorithm and other algorithms for the DDM. [Table 12](#) indicates that the best error values

**Table 11** Comparison of various algorithms and IEO for the single-diode model.

Method	$I_{ph}(A)$	$I_O$	$a$	$R_S$	$R_P$	Error	Average	Std
GA	0.7619	0.8087	1.5751	0.0299	52.3729	0.01908	0.07834	9.20E-04
PSO	8.2305	3.09E-10	1.0802	0.2422	96.8938	0.0069	0.0059	3.48E-05
WOA	8.2255	8.05E-11	1.022	0.3253	172.4225	8.50E-15	4.17E-16	1.78E-15
GWO	8.2109	5.78E-22	0.5084	0.005	43.8802	9.23E-10	2.29E-11	5.49E-11
SCA	8.2685	5.04E-27	0.4137	0.313	43.894	6.66E-14	1.73E-09	2.44E-09
MVO	8.2106	1.25E-08	1.279	0.00524	64.3523	1.02E-07	3.91E-10	1.70E-09
EO	8.2133	2.23E-08	1.3159	0.0292	72.1747	1.81E-23	5.52E-17	3.02E-16
<b>IEO</b>	<b>8.2178</b>	<b>1.02E-08</b>	<b>1.266</b>	<b>0.0709</b>	<b>74.3245</b>	<b>0</b>	<b>3.46E-29</b>	<b>1.89E-28</b>

Note:

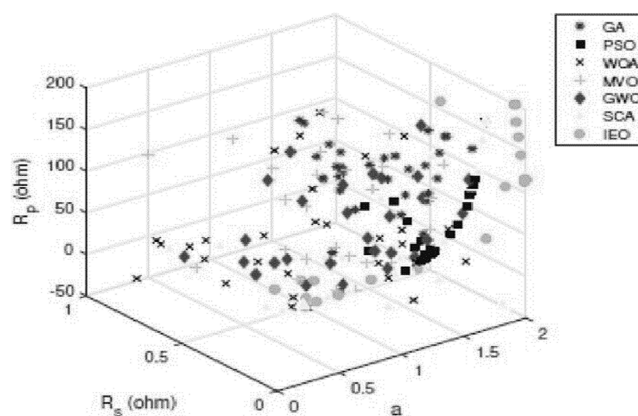
Best values shown in bold.

**Table 12** Comparison of the results of various algorithms and the IEO for the double-diode model.

Method	$I_{ph}(A)$	$I_{O1}$	$I_{O2}$	$a_1$	$a_2$	$R_S$	$R_P$	Error	Avg	Std
GA	0.8207	3.47E-09	1.13E-09	1.38	1.15	0.2633	92.64	0.0670	0.065	0.009
PSO	4.2023	2.04E-09	1.17E-10	1.21	1.07	0.17804	104.36	0.0075	0.006	8.9E-04
WOA	8.2125	3.41E-07	2.79E-11	1.82	0.99	0.0152	50.24	2.23E-14	1.2E-15	3.9E-15
GWO	8.2325	6.15E-07	1.08E-12	2	0.88	0.1416	51.58	1.08E-11	7.9E-10	4.2E-09
SCA	8.2101	1.42E-12	7.19E-06	1.22	1.67	0.0042	200	2.78E-08	4.5E-09	1.1E-08
MVO	8.2122	4.04E-07	3.97E-07	2	1.54	0.0403	149.29	1.77E-10	1.2E-09	3.1E-09
EO	8.2153	5.53E-07	3.16E-08	1.95	1.43	0.0964	149.79	5.28E-21	4.5E-18	2.4E-17
<b>IEO</b>	<b>8.2108</b>	<b>1.00E-06</b>	<b>2.32E-07</b>	<b>1.82</b>	<b>1.52</b>	<b>0.0049</b>	<b>50</b>	<b>0</b>	<b>2.8E-22</b>	<b>1.5E-21</b>

Note:

Best values shown in bold.

**Figure 12** Scatter plot of the optimal results for the single-diode model of KC200GT cell using different algorithms.  
Full-size DOI: 10.7717/peerj-cs.708/fig-12

obtained by the IEO were zero. The IEO thus achieved the best results of the six algorithms tested, followed by SCA. Whereas, GA achieved the poorest results.

To sum up the obtained results, Tables 11 and 12 indicate that PSO produces better results than GA. In addition, GWO generates fewer errors than PSO, GA, WOA, SCA, and

MVO. However, the IEO results are superior to those of all other approaches. Fig. 12 presents a comparison between the optimal results for the SDM of the KC200GT cell using different methods.

## CONCLUSIONS AND FUTURE WORK

Developing an accurate model of the PV system is an important and challenging task. To obtain an accurate model, it is necessary to determine the optimal parameters for the PV model using an effective optimization technique. The IEO algorithm is a recent optimization technique that is used for parameter extraction of the PV modules for the SDM and DDM. The IEO algorithm has various advantages, such as solution accuracy, convergence speed, and balance between analysis and exploitation. In this paper, the PV generator is modeled using the SDM and DDM, and the parameters of each model were optimally determined using the IEO algorithm. The IEO has been compared to the following six metaheuristic algorithms: GA, PSO, SCA, WOA, MVO, and GWO. The results achieved using the IEO are accurate than those achieved by the other methods. The IEO could be a good candidate for solving the optimization problem of the SC systems. In future work, the IEO can be applied to identify the PV parameters for the multi-dimension diode and multi-diode models. Moreover, it can also be used for calculating the current-voltage characteristic of the multi-diode models.

## ABBREVIATIONS

<b>PV</b>	Photovoltaic
<b>IEO</b>	Improved Equilibrium Optimizer algorithm
<b>EO</b>	Equilibrium Optimizer algorithm
<b>BL</b>	Opposition Based Learning
<b>SDM</b>	single diode model
<b>DDM</b>	double diode model
<b>RESs</b>	renewable energy sources
<b>SCs</b>	system uses solar cells
$V_{oc}$	open circuit voltage
$V_{mpp}$	voltage at the point of maximum power
$I_{mpp}$	current at the point of maximum power
$I_{sc}$	short-circuit current
$P_{mpp}$	maximum power
$K_v$	voltage temperature coefficients
$K_i$	current temperature coefficients
$I_o$	the reverse saturation current
$I_{pv}$	photogenerated current
$a$	non-physical ideality factor of the diode
$R_p$	shunt resistance
$R_s$	series resistant
<b>GA</b>	a genetic algorithm

<b>PSO</b>	particle swarm optimization
<b>SA</b>	simulated annealing
<b>GWO</b>	gray wolf optimizer
<b>FPA</b>	flower pollination algorithm
<b>MSSO</b>	simplified swarm optimization algorithm
$I_D$	The diode current
$I_{o,cell}$	The reverse saturation current of the diode
$N_c$	represents the number of cells
<b>K</b>	Boltzmann constant
<b>q</b>	charge of an electron
<b>T</b>	The temperature (in Kelvin)
$C^{initial}$	The initial condensation of the $i$ th particle
$C_{max}$	The maximum of the dimensions
$C_{min}$	The minimum of the dimensions
<b>n</b>	the particle number representing a population
<b>G</b>	key expression of the proposal technique
<b>WOA</b>	whale optimizer algorithm
<b>SCA</b>	since-cosine algorithm
<b>MVO</b>	Multi-Verse Optimizer
<b>ABC</b>	artificial bee colony
<b>WDO</b>	Wind Driven Optimization
<b>SCE</b>	Sister chromatid exchange
<b>ImCSA</b>	improved cuckoo search algorithm
<b>ISCA</b>	Interview Schedule For Children and Adolescents
<b>SMA</b>	Superior Mesenteric artery
<b>COA</b>	Coyote optimization algorithm
<b>TLO</b>	Teaching-learning-based optimization

## ADDITIONAL INFORMATION AND DECLARATIONS

### Funding

The authors received no funding for this work.

### Competing Interests

The authors declare that they have no competing interests.

### Author Contributions

- Essam H. Houssein conceived and designed the experiments, performed the experiments, analyzed the data, prepared figures and/or tables, authored or reviewed drafts of the paper, and approved the final draft.

- Gamela Nageh conceived and designed the experiments, performed the experiments, analyzed the data, performed the computation work, prepared figures and/or tables, authored or reviewed drafts of the paper, and approved the final draft.
- Mohamed Abd Elaziz conceived and designed the experiments, performed the experiments, analyzed the data, prepared figures and/or tables, authored or reviewed drafts of the paper, and approved the final draft.
- Eman Younis conceived and designed the experiments, performed the experiments, analyzed the data, prepared figures and/or tables, authored or reviewed drafts of the paper, and approved the final draft.

## Data Availability

The following information was supplied regarding data availability:

The improved code for equilibrium optimization using opposition-based learning and the code to generate simulated datasets used to test the code is available in the [Supplemental Files](#).

## Supplemental Information

Supplemental information for this article can be found online at <http://dx.doi.org/10.7717/peerj-cs.708#supplemental-information>.

## REFERENCES

- AbdElminaam DS, Said M, Houssein EH.** 2021. Turbulent flow of water-based optimization using new objective function for parameter extraction of six photovoltaic models. *IEEE Access* **9**:35382–35398.
- Alam D, Yousri D, Eteiba M.** 2015. Flower pollination algorithm based solar pv parameter estimation. *Energy Conversion and Management* **101**(9):410–422 DOI [10.1016/j.enconman.2015.05.074](https://doi.org/10.1016/j.enconman.2015.05.074).
- AlHajri M, El-Naggar K, AlRashidi M, Al-Othman A.** 2012. Optimal extraction of solar cell parameters using pattern search. *Renewable Energy* **44**(4):238–245 DOI [10.1016/j.renene.2012.01.082](https://doi.org/10.1016/j.renene.2012.01.082).
- Ali E, El-Hameed M, El-Fergany A, El-Arini M.** 2016. Parameter extraction of photovoltaic generating units using multi-verse optimizer. *Sustainable Energy Technologies and Assessments* **17**(7):68–76 DOI [10.1016/j.seta.2016.08.004](https://doi.org/10.1016/j.seta.2016.08.004).
- AlRashidi M, AlHajri M, El-Naggar K, Al-Othman A.** 2011. A new estimation approach for determining the I-V characteristics of solar cells. *Solar Energy* **85**(7):1543–1550 DOI [10.1016/j.solener.2011.04.013](https://doi.org/10.1016/j.solener.2011.04.013).
- Askarzadeh A, Rezazadeh A.** 2012. Parameter identification for solar cell models using harmony search-based algorithms. *Solar Energy* **86**(11):3241–3249 DOI [10.1016/j.solener.2012.08.018](https://doi.org/10.1016/j.solener.2012.08.018).
- Askarzadeh A, Rezazadeh A.** 2013a. Artificial bee swarm optimization algorithm for parameters identification of solar cell models. *Applied Energy* **102**:943–949 DOI [10.1016/j.apenergy.2012.09.052](https://doi.org/10.1016/j.apenergy.2012.09.052).
- Askarzadeh A, Rezazadeh A.** 2013b. Extraction of maximum power point in solar cells using bird mating optimizer-based parameters identification approach. *Solar Energy* **90**(7):123–133 DOI [10.1016/j.solener.2013.01.010](https://doi.org/10.1016/j.solener.2013.01.010).

- Bagher AM, Vahid M, Mohsen M, Parvin D.** 2015. Hydroelectric energy advantages and disadvantages. *American Journal of Energy Science* 2(2):17.
- Biswas PP, Suganthan P, Wu G, Amaralunga GA.** 2019. Parameter estimation of solar cells using datasheet information with the application of an adaptive differential evolution algorithm. *Renewable energy* 132(1):425–438 DOI 10.1016/j.renene.2018.07.152.
- Chan D, Phillips J, Phang J.** 1986. A comparative study of extraction methods for solar cell model parameters. *Solid-State Electronics* 29(3):329–337 DOI 10.1016/0038-1101(86)90212-1.
- Chellaswamy C, Ramesh R.** 2016. Parameter extraction of solar cell models based on adaptive differential evolution algorithm. *Renewable Energy* 97(12):823–837 DOI 10.1016/j.renene.2016.06.024.
- Chen H, Jiao S, Heidari AA, Wang M, Chen X, Zhao X.** 2019. An opposition-based sine cosine approach with local search for parameter estimation of photovoltaic models. *Energy Conversion and Management* 195:927–942 DOI 10.1016/j.enconman.2019.05.057.
- Chin CS, Neelakantan P, Yang SS, Chua BL, Tze Kin Teo K.** 2011. Effect of partially shaded conditions on photovoltaic array's maximum power point tracking. *International Journal of Simulation-Systems, Science & Technology* 12(3):1–8.
- Dai C, Chen W, Zhu Y.** 2009. Seeker optimization algorithm for digital IIR filter design. *IEEE Transactions on Industrial Electronics* 57(5):1710–1718.
- Derick M, Rani C, Rajesh M, Farrag M, Wang Y, Busawon K.** 2017. An improved optimization technique for estimation of solar photovoltaic parameters. *Solar Energy* 157(11):116–124 DOI 10.1016/j.solener.2017.08.006.
- Diab AAZ, Sultan HM, Do TD, Kamel OM, Mossa MA.** 2020. Coyote optimization algorithm for parameters estimation of various models of solar cells and pv modules. *IEEE Access* 8:111102–111140 DOI 10.1109/ACCESS.2020.3000770.
- Dunn S.** 2002. Hydrogen futures: toward a sustainable energy system. *International Journal of Hydrogen Energy* 27(3):235–264 DOI 10.1016/S0360-3199(01)00131-8.
- Easwarakhanthan T, Bottin J, Bouhouc I, Boutrit C.** 1986. Nonlinear minimization algorithm for determining the solar cell parameters with microcomputers. *International Journal of Solar Energy* 4(1):1–12 DOI 10.1080/01425918608909835.
- Egbert G, Ray R.** 2000. Significant dissipation of tidal energy in the deep ocean inferred from satellite altimeter data. *Nature* 405(6788):775–778 DOI 10.1038/35015531.
- El-Arini MM, Othman AM, Fathy A.** 2013. A new optimization approach for maximizing the photovoltaic panel power based on genetic algorithm and lagrange multiplier algorithm. *International Journal of Photoenergy* 2013(1):1–12 DOI 10.1155/2013/481468.
- El-Fergany A.** 2015. Efficient tool to characterize photovoltaic generating systems using mine blast algorithm. *Electric Power Components and Systems* 43(8–10):890–901 DOI 10.1080/15325008.2015.1014579.
- El-Naggar KM, AlRashidi M, AlHajri M, Al-Othman A.** 2012. Simulated annealing algorithm for photovoltaic parameters identification. *Solar Energy* 86(1):266–274 DOI 10.1016/j.solener.2011.09.032.
- Faramarzi A, Heidarnejad M, Stephens B, Mirjalili S.** 2020. Equilibrium optimizer: a novel optimization algorithm. *Knowledge-Based System* 191:105190 DOI 10.1016/j.knosys.2019.105190.
- Gao X, Cui Y, Hu J, Xu G, Wang Z, Qu J, Wang H.** 2018. Parameter extraction of solar cell models using improved shuffled complex evolution algorithm. *Energy Conversion and Management* 157:460–479 DOI 10.1016/j.enconman.2017.12.033.

- Gong W, Cai Z.** 2013. Parameter extraction of solar cell models using repaired adaptive differential evolution. *Solar Energy* **94**(0):209–220 DOI [10.1016/j.solener.2013.05.007](https://doi.org/10.1016/j.solener.2013.05.007).
- Gotmare A, Bhattacharjee SS, Patidar R, George NV.** 2017. Swarm and evolutionary computing algorithms for system identification and filter design: a comprehensive review. *Swarm and Evolutionary Computation* **32**(e40549):68–84 DOI [10.1016/j.swevo.2016.06.007](https://doi.org/10.1016/j.swevo.2016.06.007).
- Hocaoglu FO.** 2011. Stochastic approach for daily solar radiation modeling. *Solar Energy* **85**(2):278–287.
- Houssein EH.** 2019. Machine learning and meta-heuristic algorithms for renewable energy: a systematic review. In: *Advanced Control and Optimization Paradigms for Wind Energy Systems*. Berlin: Springer, 165–187.
- Humada AM, Hojabri M, Mekhilef S, Hamada HM.** 2016. Solar cell parameters extraction based on single and double-diode models: a review. *Renewable and Sustainable Energy Reviews* **56**:494–509 DOI [10.1016/j.rser.2015.11.051](https://doi.org/10.1016/j.rser.2015.11.051).
- Ismaeel AA, Houssein EH, Oliva D, Said M.** 2021. Gradient-based optimizer for parameter extraction in photovoltaic models. *IEEE Access* **9**:13403–13416 DOI [10.1109/ACCESS.2021.3052153](https://doi.org/10.1109/ACCESS.2021.3052153).
- Ismail MS, Moghavvemi M, Mahlia T.** 2013. Characterization of pv panel and global optimization of its model parameters using genetic algorithm. *Energy Conversion and Management* **73**:10–25 DOI [10.1016/j.enconman.2013.03.033](https://doi.org/10.1016/j.enconman.2013.03.033).
- Jacob B, Balasubramanian K, Azharuddin SM, Rajasekar N.** 2015. Solar pv modelling and parameter extraction using artificial immune system. *Energy Procedia* **75**:331–336 DOI [10.1016/j.egypro.2015.07.375](https://doi.org/10.1016/j.egypro.2015.07.375).
- Kang T, Yao J, Jin M, Yang S, Duong T.** 2018. A novel improved cuckoo search algorithm for parameter estimation of photovoltaic (pv) models. *Energies* **11**(5):1060.
- Kumar C, Raj TD, Premkumar M, Raj TD.** 2020. A new stochastic slime mould optimization algorithm for the estimation of solar photovoltaic cell parameters. *Optik* **223**:165277.
- Li S, Gong W, Yan X, Hu C, Bai D, Wang L, Gao L.** 2019. Parameter extraction of photovoltaic models using an improved teaching-learning-based optimization. *Energy Conversion and Management* **186**:293–305.
- Lim LHI, Ye Z, Ye J, Yang D, Du H.** 2015. A linear identification of diode models from single *i-v* characteristics of pv panels. *IEEE Transactions on Industrial Electronics* **62**(7):4181–4193.
- Lin P, Cheng S, Yeh W, Chen Z, Wu L.** 2017a. Parameters extraction of solar cell models using a modified simplified swarm optimization algorithm. *Solar Energy* **144**:594–603.
- Lin P, Cheng S, Yeh W, Chen Z, Wu L.** 2017b. Parameters extraction of solar cell models using a modified simplified swarm optimization algorithm. *Solar Energy* **144**(11):594–603 DOI [10.1016/j.solener.2017.01.064](https://doi.org/10.1016/j.solener.2017.01.064).
- López PR, Jurado F, Reyes NR, Galán SG, Gómez M.** 2008. Particle swarm optimization for biomass-fuelled systems with technical constraints. *Engineering Applications of Artificial Intelligence* **21**(8):1389–1396 DOI [10.1016/j.engappai.2008.04.013](https://doi.org/10.1016/j.engappai.2008.04.013).
- Mathew D, Rani C, Kumar MR, Wang Y, Binns R, Busawon K.** 2017. Wind-driven optimization technique for estimation of solar photovoltaic parameters. *IEEE Journal of Photovoltaics* **8**(1):248–256 DOI [10.1109/JPHOTOV.2017.2769000](https://doi.org/10.1109/JPHOTOV.2017.2769000).
- Munshi AA, Yasser A-RM.** 2017. Comparisons among bat algorithms with various objective functions on grouping photovoltaic power patterns. *Solar Energy* **144**(2):254–266 DOI [10.1016/j.solener.2017.01.034](https://doi.org/10.1016/j.solener.2017.01.034).

- Navabi R, Abedi S, Hosseinian SH, Pal R.** 2015. On the fast convergence modeling and accurate calculation of pv output energy for operation and planning studies. *Energy Conversion and Management* **89**(2):497–506 DOI [10.1016/j.enconman.2014.09.070](https://doi.org/10.1016/j.enconman.2014.09.070).
- Oliva D, El Aziz MA, Hassanien AE.** 2017. Parameter estimation of photovoltaic cells using an improved chaotic whale optimization algorithm. *Applied Energy* **200**:141–154 DOI [10.1016/j.apenergy.2017.05.029](https://doi.org/10.1016/j.apenergy.2017.05.029).
- Oliva D, Elaziz MA, Elsheikh AH, Ewees AA.** 2019. A review on meta-heuristics methods for estimating parameters of solar cells. *Journal of Power Sources* **435**:126683 DOI [10.1016/j.jpowsour.2019.05.089](https://doi.org/10.1016/j.jpowsour.2019.05.089).
- Oliva D, Ewees AA, Aziz MAE, Hassanien AE, Pérez-Cisneros M.** 2017. A chaotic improved artificial bee colony for parameter estimation of photovoltaic cells. *Energies* **10**(7):865 DOI [10.3390/en10070865](https://doi.org/10.3390/en10070865).
- Osama S, Darwish A, Houssein EH, Hassanien AE, Fahmy AA, Mahrous A.** 2017. Long-term wind speed prediction based on optimized support vector regression. In: *2017 Eighth International Conference on Intelligent Computing and Information Systems (ICICIS)*. Piscataway: IEEE, 191–196.
- Osheba DS, Azazi HZ, Shokralla S.** 2017. Parameter estimation of a photovoltaic array using direct search optimization algorithm. *Journal of Renewable and Sustainable Energy* **9**(4):43501 DOI [10.1063/1.4995270](https://doi.org/10.1063/1.4995270).
- Park J, Kim HG, Cho Y, Shin C.** 2014. Simple modeling and simulation of photovoltaic panels using matlab/simulink. *Advanced Science and Technology Letters* **73**:147–155.
- Rodrguez AS, Murillo EC.** 2017. Automatic parametrization of support vector machines for short texts polarity detection. *CLEI Electronic Journal* **20**(1):6.
- Salam Z, Ishaque K, Taheri H.** 2010. An improved two-diode photovoltaic (pv) model for pv system. In: *2010 Joint International Conference on Power Electronics, Drives and Energy Systems & 2010 Power India*. Piscataway: IEEE, 1–5.
- Siddiqui M, Abido M.** 2013. Parameter estimation for five-and seven-parameter photovoltaic electrical models using evolutionary algorithms. *Applied Soft Computing* **13**(12):4608–4621 DOI [10.1016/j.asoc.2013.07.005](https://doi.org/10.1016/j.asoc.2013.07.005).
- Tizhoosh HR.** 2005. Opposition-based learning: a new scheme for machine intelligence. In: *International Conference on Computational Intelligence for Modelling, Control and Automation Agents, Web Technologies and Internet Commerce (CIMCA-IAWTIC'06)*. Piscataway: IEEE, 695–701.
- Wei H, Cong J, Lingyun X, Deyun S.** 2011. Extracting solar cell model parameters based on chaos particle swarm algorithm. In: *2011 International Conference on Electric Information and Control Engineering*. Piscataway: IEEE, 398–402.
- Yuan X, Xiang Y, He Y.** 2014. Parameter extraction of solar cell models using mutative-scale parallel chaos optimization algorithm. *Solar Energy* **108**(3):238–251 DOI [10.1016/j.solener.2014.07.013](https://doi.org/10.1016/j.solener.2014.07.013).